iScience

CellPress
OPEN ACCESS

Article

Battery lifetime prediction and performance assessment of different modeling approaches

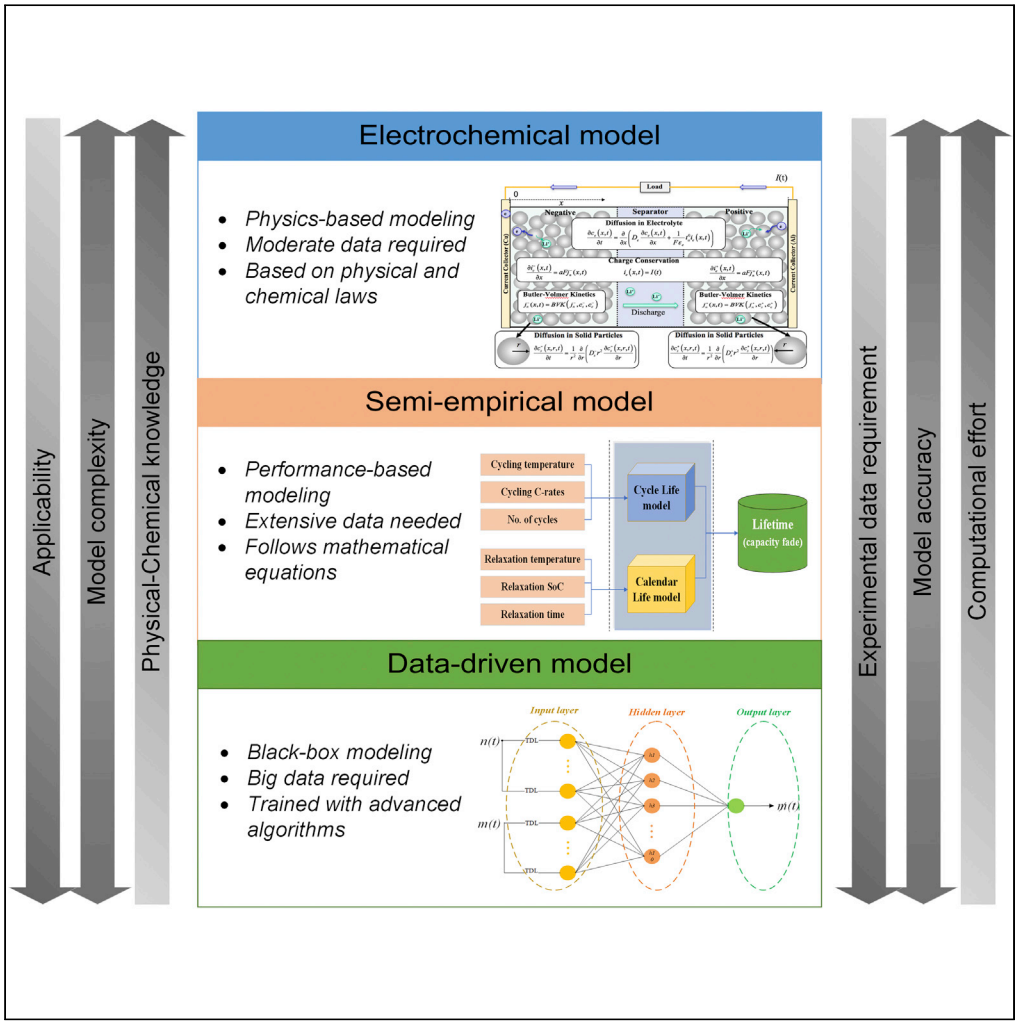

Md Sazzad Hosen, Joris Jaguemont, Joeri Van Mierlo, Maitane Berecibar

md.sazzad.hosen@vub.be

HIGHLIGHTS

Development of several lifetime models based on long-term cell aging dataset

Models validation by WLTC cycling and based on realistic scenarios

Models assessment in terms of accuracy, computational effort, applicability, etc.

Pros and cons of the best lifetime model toward realistic use

Hosen et al., iScience 24, 102060
February 19, 2021
https://doi.org/10.1016/j.isci.2021.102060

iScience

CellPress
OPEN ACCESS

Article

Battery lifetime prediction and performance assessment of different modeling approaches

Md Sazzad Hosen,[1,2,3,*] Joris Jaguemont,[1,2] Joeri Van Mierlo,[1,2] and Maitane Berecibar[1,2]

SUMMARY

Lithium-ion battery technologies have conquered the current energy storage market as the most preferred choice thanks to their development in a longer lifetime. However, choosing the most suitable battery aging modeling methodology based on investigated lifetime characterization is still a challenge. In this work, a comprehensive aging dataset of nickel-manganese-cobalt oxide (NMC) cell is used to develop and/or train different capacity fade models to compare output responses. The assessment is conducted for semi-empirical modeling (SeM) approach against a machine learning model and an artificial neural network model. Among all, the nonlinear autoregressive network (NARXnet) can predict the capacity degradation most precisely minimizing the computational effort as well. This research work signifies the importance of lifetime methodological choice and model performance in understanding the complex and nonlinear Li-ion battery aging behavior.

INTRODUCTION

Lithium-ion (Li-ion) batteries have become an integral part of our daily electronics devices and the state-of-the-art choice of e-mobility (Scrosati and Garche, 2010; Hu et al., 2017). The electrification of the automotive sector following the global CO_2 footprint has been made possible because of the continuous development of Li-ion batteries (Nykvist and Nilsson, 2015). However, the challenge of extending the battery life and having a reliable and long-lasting battery system is still the bottleneck in expanding the electric vehicle (EV) fleet. Substantial research has been conducted during the last decade to identify the degradation mechanisms of different Li-ion technologies to further accelerate battery development and overcome the range anxiety (Barré et al., 2013; Birkl et al., 2017). Lithium batteries degrade over time within or without operation most commonly termed as battery cycle life (charge/discharge) and calendar life (rest/storage), respectively (Palacín, 2018). While in use, a battery undergoes plenty of charge-discharge cycles from shallow to full depth along with several other operating conditions, which result either in capacity fade and/or internal resistance (IR) growth. Moreover, the storage or rest period of a battery over the lifetime is also significant, although the degradation impact is lesser, comparatively (de Hoog et al., 2017). The diversified and interconnected aging mechanisms result in the nonlinear degradation process during the lifetime (Birkl et al., 2017; Palacín, 2018). The different stress factors contributing to battery aging have varying limits of degradation impacts, while accelerated and unexpected events can also lead to faster battery failure (Palacín and Guibert, 2016).

Battery life has been a crucial subject of investigation since its introduction to the commercial vehicle, during which different Li-ion batteries are cycled and/or stored to identify the degradation mechanisms separately (Käbitz et al., 2013; Ecker et al., 2014) or together. Most commonly laboratory-level tests are performed to understand the battery aging behavior under different operating conditions, and then the generated data are either fed or used to develop lifetime models. The performance-based predictive models are often built with fitting mathematical equations or trained with advanced algorithms such as machine learning (ML), etc. (Berecibar et al., 2016; Li et al., 2019). These different modeling approaches can forecast the whole life in terms of battery capacity fade and/or IR growth (Jafari et al., 2018; Hu et al., 2020). However, the model performance heavily relies on the quality and quantity of the investigated dataset and the selection of the modeling methodology. The performance-based and black box models require little or no knowledge of the battery chemistries, but a significant amount of characterization data is

[1]Battery Innovation Center, MOBI Research Group, Vrije Universiteit Brussel, Pleinlaan 2, 1050 Brussels, Belgium

[2]Flanders Make, 3001 Heverlee, Belgium

[3]Lead contact

*Correspondence: md.sazzad.hosen@vub.be

https://doi.org/10.1016/j.isci.2021.102060

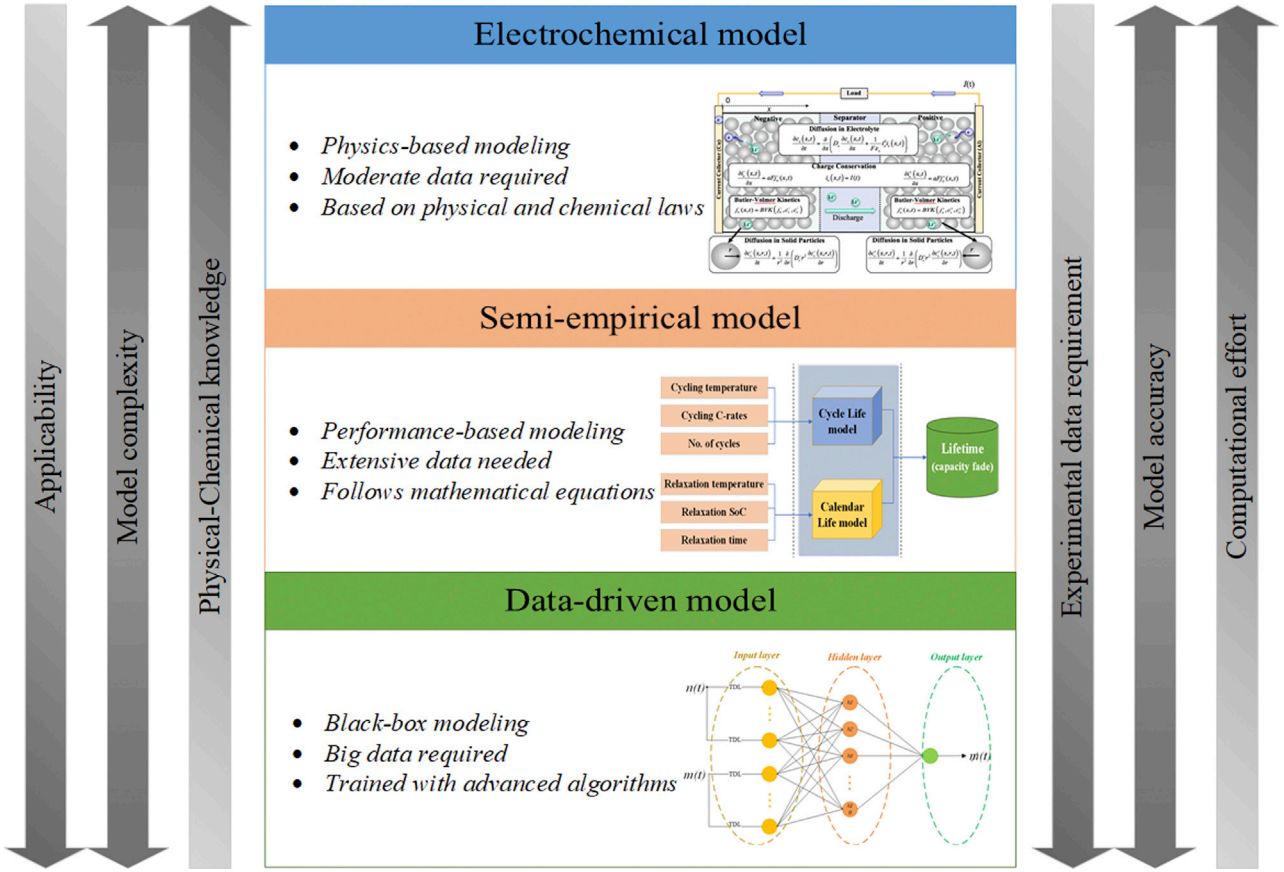

Figure 1. Battery lifetime modeling methodologies at a glance

The darker shades in the arrows refer to more intensity. The figure in the top panel is adapted from (He et al., 2018).

necessary to outline the model response (Lucu et al., 2018). On the contrary, battery physics-based models can identify the loss of lithium inventory and active materials by analyzing the key degradation mechanisms such as solid-electrolyte interphase, lithium plating, etc. (Christensen and Newman, 2005; Yang et al., 2017; He et al., 2018). Figure 1 illustrates the comparison of different lifetime modeling methodologies. In this research work, model development and assessment are investigated focusing on the less complex and performance-based methodologies, which include the semi-empirical approach and ML algorithms. The objective is to evaluate the developed data-driven model methodologies that are constructed from a commercial cell aging dataset and can be implemented in real life.

Performance-dependent semi-empirical aging models based on characteristic results are usually developed and parameterized from long-term lifetime tests (Omar et al., 2014) or accelerated tests (Ecker et al., 2012). An extensive range of investigation covering crucial cycling parameters of temperature, depth of discharge (DoD), state of charge (SoC), charge-discharge rate (C-rate), ampere-hour throughput, cycle number, etc., and calendar life conditions of storage temperature, storage SoC, storage duration, etc., are often used to characterize the battery lifetime (Dai et al., 2013; Su et al., 2016; Ecker et al., 2017). The performance of the constructed model is then evaluated with regular cycling or real-life profiles, i.e., worldwide harmonized light-duty test cycle (WLTC) by comparing the simulated capacity and power fade against actual measurement (Suri and Onori, 2016; de Hoog et al., 2018; Li et al., 2018). The crucial limitation of semi-empirical aging models is the prediction accuracy, while the fitting response on unknown profiles depends on the quality of the generated dataset. Moreover, the operating conditions of the investigated data act as an optimal boundary criterion of this methodology beyond which the prediction response accuracy is compromised.

The development of data-driven methodologies can improve the modeling accuracy significantly by compromising the simplicity of model construction and computational effort (Lucu et al., 2018; Li et al.,

2019). Data-driven models have been a preferred choice in estimating battery state of health and remaining useful life (Saha et al., 2007; Richardson et al., 2017; Li et al., 2018), but recently, it has gained popularity in lifetime prediction as well thanks to its high accuracy (Liu et al., 2020; Lucu et al., 2020). However, both the quality and quantity of the training dataset are prerequisites in this methodology, absence of any of which may impact the model accuracy and effectiveness (Severson et al., 2019). Among the data-driven models support vector machine, regression algorithms, ensembled models, etc., are regularly used in the field of battery aging (Nuhic et al., 2013; Xing et al., 2013; Liu et al., 2019). The Gaussian process (GP) regression (GPR) has been identified as a promising prospect thanks to its nonparametric and probabilistic characteristics (Liu et al., 2013; Richardson et al., 2019). Moreover, advanced algorithms like artificial neural network (ANN) mimicking neurons in the biological system is employed for pattern recognition in battery health prediction (Liu et al., 2010; Eddahech et al., 2012; Wu et al., 2016). However, ANN is not employed in the full battery life prediction without initial data. One of the promising ANN networks as nonlinear autoregressive with exogenous input (NARX) is considered to be quite accurate for dynamic systems and has been used to develop battery degradation models (Hussein, 2015; Member and Ibe-ekeocha, 2017). Although using advanced modeling techniques may improve predictive model accuracy, the selection of a suitable algorithm is not straightforward especially for a complex nonlinear system like batteries. Furthermore, the rationalization of the performance of different models and algorithms is impractical unless identical training data are utilized. One of the most common and free datasets is provided by NASA Ames Prognostic Center of Excellence (Saha and Goebel, 2007), which has been regularly used by researchers for battery health prognosis (Cheng et al., 2015; Wang and Mamo, 2018; Wang et al., 2019). In lifetime modeling, public data repositories (Severson et al., 2019) and data from European projects (Batteries2020) (de Hoog et al., 2017) are considered to model the cycle life in separate literature (Zhu et al., 2019; Lucu et al., 2020). However, the output response of the degradation models is usually methodology-dependent and based on a set of specific input parameters. Thus, developing different model types by using a single dataset and a specific set of stress factors is a rare and challenging task that can facilitate a proper model performance comparison.

In this research work, the authors have developed a neural network (NARX) model and adapted their developed semi-empirical (SeM) and data-driven (GPR) models using an in-house-generated comprehensive dataset of 40 nickel-manganese-cobalt oxide (NMC) cells. The novel comparison of different performance-based models constructing all of them from a single dataset is done for the first time. The detailed model assessment can clarify the choice of different modeling methodologies helping the original equipment manufacturers to implement the most suitable approaches. Further in this article, the experimental arrangement is briefly explained in the following section. After that, the model construction process is described for the selected techniques. The developed models are then validated with static and dynamic current profiles and assessed, and the performances are compared. Finally, the work is concluded providing remarks on choosing the most suitable modeling methodology for battery lifetime prediction.

Lifetime model development

Aging characteristics and data processing

The prerequisite of any performance-based model development includes detailed analysis and pre-processing of the generated data. Thus, the stress factors are analyzed to understand the battery degradation behavior. Figure 2 shows the capacity fade of different cells that are cycled following the test flow displayed in Figure S1. Figure S1 is related to the studied lifetime cycling and relaxation procedure to degrade the battery. The results indicate that the capacity decay is significantly dependent on the cycling temperature (cell surface) irrespective of the relaxation temperature. The aging is also affected by the storage SoC especially at room temperature. The authors have thoroughly investigated all the crucial impact factors and have identified the following parameters that contribute to the total capacity fade.

- Cycling parameters: number of cycles, temperature, and C-rates for charge and discharge direction.
- Calendar aging parameters: rest temperature and rest SoC.

Relaxation time is found to have no clear effect on degradation but is still considered to have common parameterization. While going forward to the model development phase, all these parameters are considered to maintain a common platform to justify the comparison among the adapted model performance.

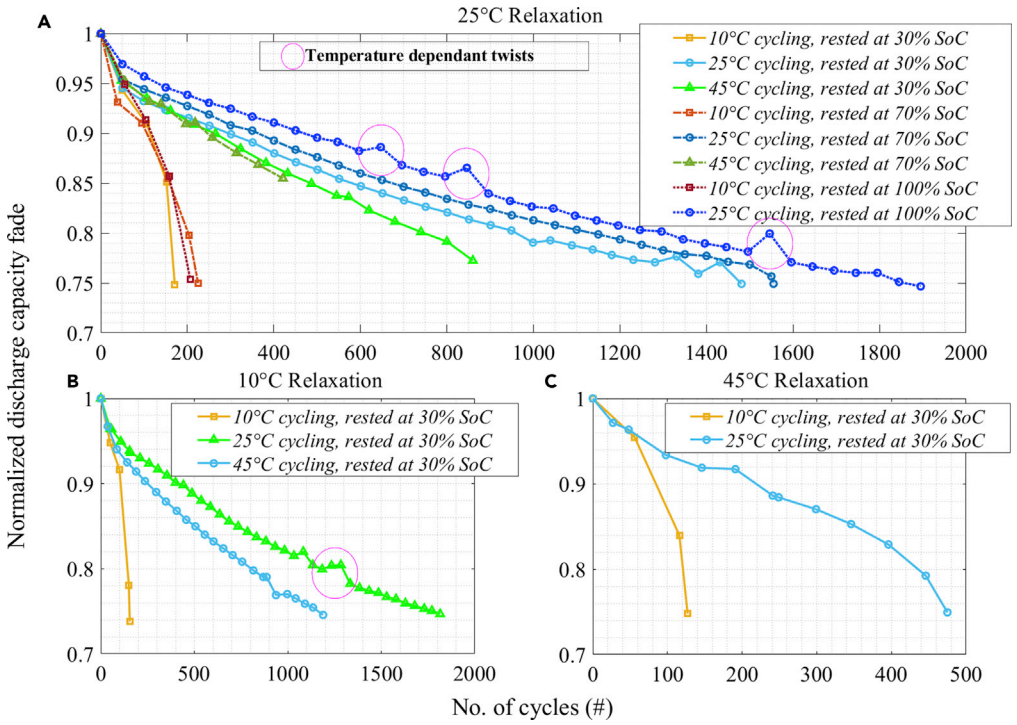

Figure 2. The capacity degradation of different cycling scenarios with 1C charge-discharge rate and relaxed for 5 days after every round

(A–C) (A) Room temperature relaxation at various rest SoC, (B) 10°C relaxation at 30% SoC, and (C) 45°C relaxation at 30% SoC.

Semi-empirical model

This type of statistical model merely depends on diverse battery characteristics and contexts. A wide range of operating condition results are manifested with mathematical equations simplifying different degradation aspects. Authors have developed such a parameterized model for NMC batteries in their previous research, which has been validated for different dynamic applications (Hosen et al., 2020). The baseline of the model is adapted for the investigated cell in this work, and the outline framework is depicted in Figure 3. The developed model consists of two main sections separated by cycle life and calendar life contributions to total degradation.

Battery cycle life deteriorates over time as it is impacted by multiple factors and interconnected degradation mechanisms (Birkl et al., 2017; Palacín, 2018). Thus the variation of cycling operating conditions plays a vital role in identifying the influential parameters. In the investigated campaign, NMC cells are cycled within the entire voltage range meaning the full DoD is utilized during charge-discharge over the first life period. So, the number of cycles (NoC) is considered as the common parameter, while the cycling ambient temperature (10°C, 25°C, and 45°C) and the C-rate (0.33C, 1C, and 2C) are other crucial variables. The cycling capacity degradation can be expressed as the following general equation:

$$\text{Cycling capacity loss}\,(\text{NoC},\alpha) = \sum_{i=0,j=0}^{n,m}\left(A_i * (NoC)^i + B_j * (\alpha)^j\right) \qquad \text{(Equation 1)}$$

In Equation (1), A_i and B_j are constant coefficients, n and m are orders of the 3D surface fit equation, and α represents either the cycling operating temperature or the C-rates. The coefficients and the surface fit orders are for the X and Y axes, respectively. This cycling degradation equation is formulated from in-house NMC battery datasets generated in Batteries2020 (Batteries2020, 2013) and BATTLE (BATTLE, 2013) projects and adapted for the investigated NMC cell, whereas the calendar life capacity fade fitting equations are inherited from the author's previous work (Hosen et al., 2020). The polynomials are represented by Arrhenius equation and the fitting equations relating the calendar life capacity fade to the function of the temperature, SoC, and time. The Arrhenius equation is used to fit the relaxation data to identify the aging rate

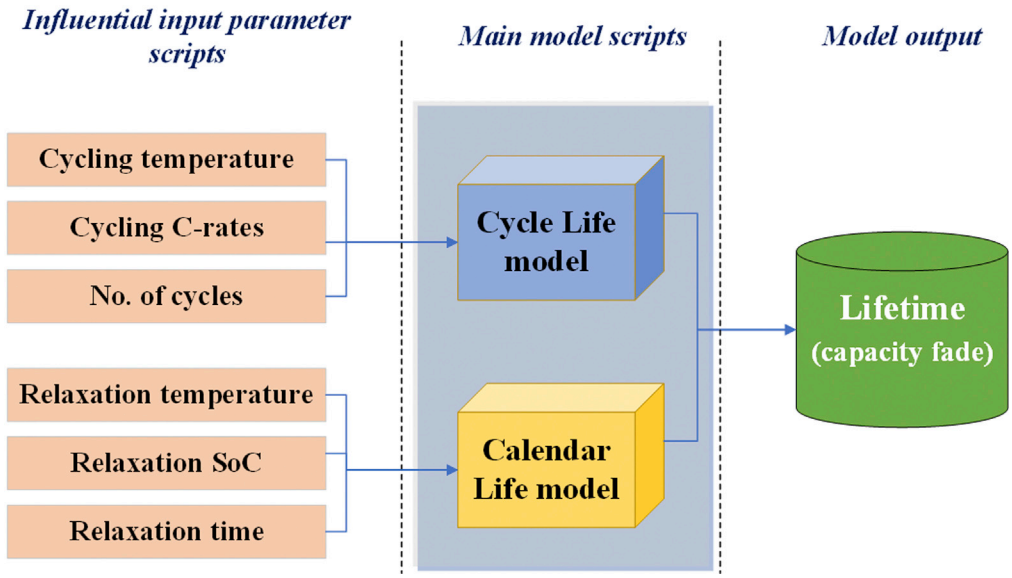

Figure 3. The developed semi-empirical model framework

dependency at different temperatures, which is common in the literature (Broussely et al., 2001). To add the impact of the storage SoC, Equation (3) is used as a surface fitting equation. Both the contributions are then summed up to have the total calendar life capacity fade.

$$\text{Calendaring degradation}_1\ (\text{Temperature}) = a * \exp\frac{-E_a}{R * Temperature} \quad \text{(Equation 2)}$$

$$\text{Calendaring degradation}_2\ (\text{time},\ \text{SoC}) = x * (time)^y * (SoC)^z + \check{z} * time * SoC \quad \text{(Equation 3)}$$

In Equations (2 and 3), a, x, y, z, and ž are coefficients; E_a is the activation energy, and R is the gas constant. In the case of the dynamic profile analysis, the current is first separated by zero and non-zero events to analyze the load and no-load situations, respectively, by the main model scripts (Figure 3). These events are then processed by different influential scripts quantifying the resultant capacity drop. For the investigated dataset, the additional relaxation phases are input to the calendar life model so that the total capacity fade can include all the considerable aspects. In this methodology, a theoretical pure cycling capacity fade can be quantified by subtracting the calendar life results from total degradation as the latter includes calendar life impact during cycling as well. MATLAB platform is used to develop the robust model with several ensembled scripts.

Gaussian process regression model

The GPR is a Bayesian probabilistic ML method (Rasmussen, 2003) that has recently been used in lifetime prognosis due to its flexible and non-parametric nature (Liu et al., 2020; Lucu et al., 2020). The highly nonlinear battery behavior during lifetime is sensitive to GPR performance; however, a suitable kernel and high-quality data could confirm stable response resulting in lower prediction error. The authors employed several different kernels to train the dataset and found the exponential kernel to be the best fit, thus it has been implemented to construct the robust lifetime model using the GPR. Figure 4 displays the excellent distribution of the predicted data to the actual cell degradation by the GP. The GP is defined as a probabilistic distribution function and in relation with mean and covariance functions as the following equations:

$$m(x) = \acute{E}(f(x)) \quad \text{(Equation 4)}$$

$$k(x, x') = \acute{E}[(f(x) - m(x)) * (f(x') - m(x'))] \quad \text{(Equation 5)}$$

$$f(x) \sim GP(m(x), k(x, x')) \quad \text{(Equation 6)}$$

In Equations (4–6), $\acute{E}$ is the expected value, although mean $m(x)$ is considered as a constant basis function. Kernel function $k(x,x')$ explains the relevant difference between the predictive response and the actual capacity. The covariance function or the kernel is the most crucial part of a GPR model, but there is no

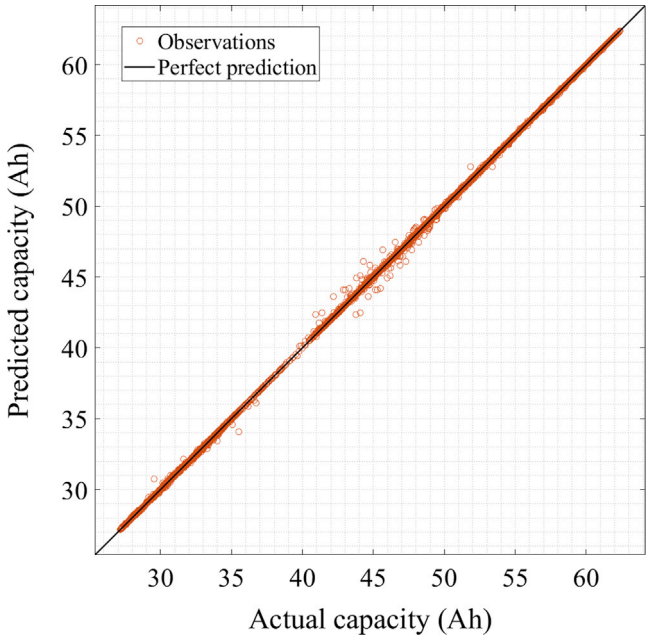

Figure 4. Trained GPR model prediction responses with the exponential kernel

standardized selection process (Duvenaud et al., 2013). However, using the exponential kernel, the model is trained with the complete dataset by selecting eight degradation features. They include cycling cell surface temperatures (charge-discharge) and C-rates during charge-discharge, the number of cycles, rest temperature, rest SoC, and the rest time. These features are formatted from the huge battery dataset as a pre-processing step to prepare the training dataset. Although the data processing and the model training took significant computational effort, remarkable prediction accuracy could be achieved by GPR. This constructed and already validated ML model is compared in this work together with the other developed models for better evaluation.

Artificial neural network model

In this work, a recurrent neural network (RNN) type architecture is used to develop the lifetime model. For a highly nonlinear system like batteries, a nonlinear autoregressive dynamic network with external inputs (NARX) can be very suitable, and it has been used for time series modeling as well (Boussaada et al., 2018; Lipu and Member, 2018). A standard feedforward NARX network (NARXnet) is used to predict the output response through regression of past output and exogenous input values. The NARX model output can be formulated as the following equation:

$$m(t) = F[m(t-1), m(t-2), \ldots, m(t-y_m), n(t-1), n(t-2), \ldots, n(t-y_n)] \quad \text{(Equation 7)}$$

In Equation (7), *F[]* is the mapping function of the *m(t)* output response that is regressed by the previous series values and past values of exogenous input data *(n)* and y_m and y_n are time delays, respectively. A double-layered open-loop feedforward neural network is selected for the modeling framework because of 2-fold reasons. First, the true past values are available for the time series, which are quite accurate to be used as the input of the network. Second, purely feedforward architecture enables the use of static backpropagation training. Figure 5 shows the selected NARXnet with tapped-delay lines and the detailed diagram.

Under this framework, the NARXnet is trained with the same eight input parameters (used in the GPR model training) by a training algorithm. Levenberg-Marquardt (LM) is used in this case as it requires less memory meaning very low computational effort. Compared with LM, Bayesian Regularization trains the model in 44 s providing a slight improvement in the performance. Ten hidden neurons are used in the NARXnet and the training, validation, and testing percentile of data are used as 90%, and 5% each, respectively. The validation data is used to evaluate the network generalization, and when it stops improving the training is stopped. The testing of the network is an independent measurement during and after training which has

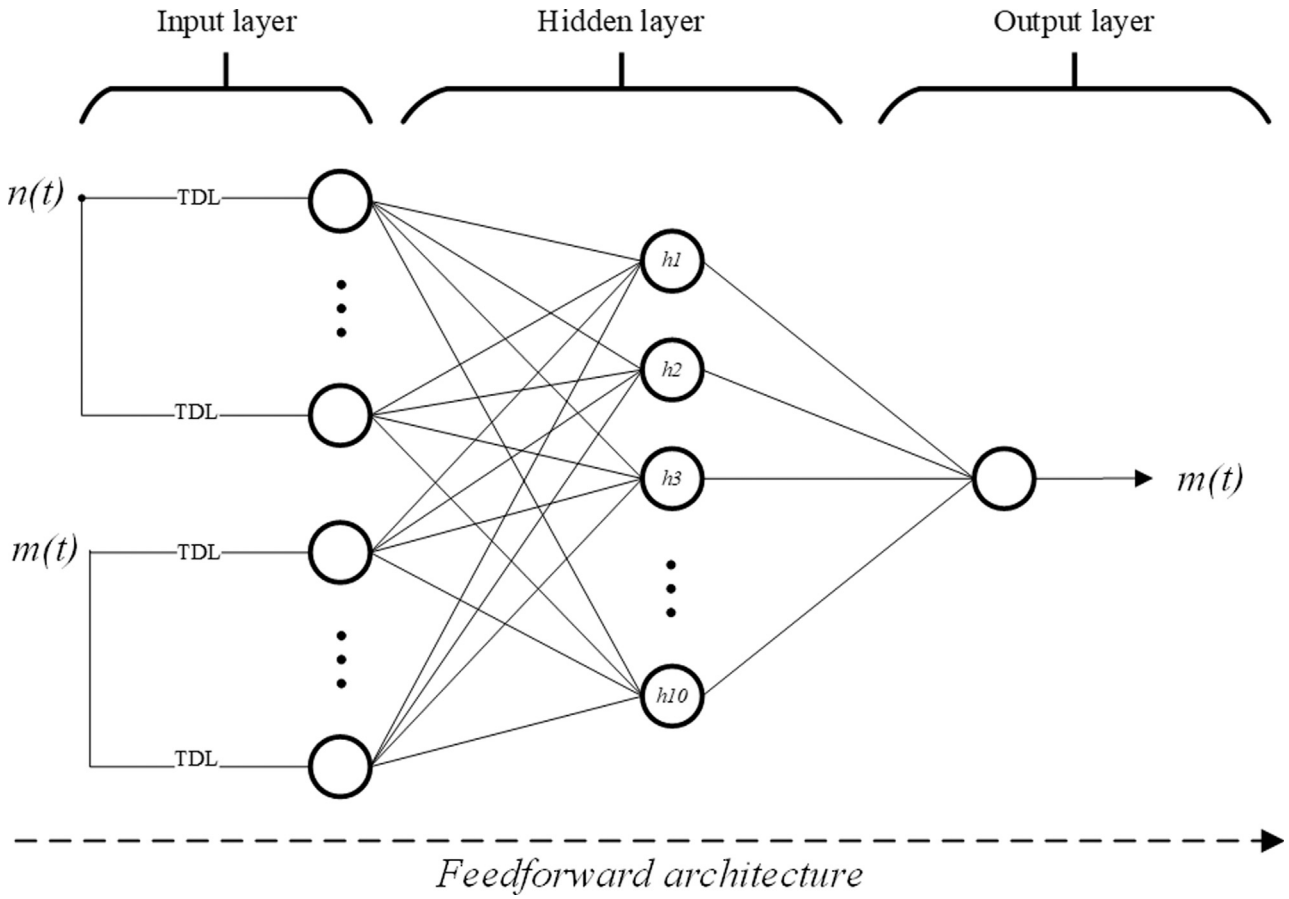

Figure 5. The developed NARXnet model structure

no impact on the process. All the training, validation, and testing processes are performed using the MATLAB environment.

Model evaluation metrics

To assess the model performances, it is necessary to define evaluation metrics. In this work, a couple of metrics are used to compare the type of models that are constructed. The error calculations are based on model prediction in terms of capacity values or capacity fade, which is compared with the actual measurement (Li et al., 2018).

$$\text{Root} - \text{mean} - \text{squared error}\left(\text{RMSE}\right) = \sqrt{\frac{1}{n}\sum_{i=1}^{n}(\Upsilon - \Psi)^2} \qquad \text{(Equation 8)}$$

$$\text{Mean} - \text{absolute error}\left(\text{MAE}\right) = \frac{1}{n}\sum_{i=1}^{n}|\Upsilon - \Psi| \qquad \text{(Equation 9)}$$

In Equations (8) and (9), n is the number of samples, i denotes n number of iterations, ψ is the actual discharge capacity, and Υ is the model output response. RMSE is commonly used and it compares the difference between the measured response to the predicted value by putting weight into it. It emphasizes the deviation and assesses the prediction performance. On the other hand, MAE can be defined as the absolute and average error of all the predicted samples. The identical weight of all the calculated errors means the prediction accuracy corresponds to smaller MAE values. Both these metrics are used for performance comparison as there is no perfect fitting that exists. For evaluation purposes, the lower the RMSE value the better and MAE is the best when the value is close to zero. To have an acceptable target range of the model's performance, less than 1 RMSE should be achieved.

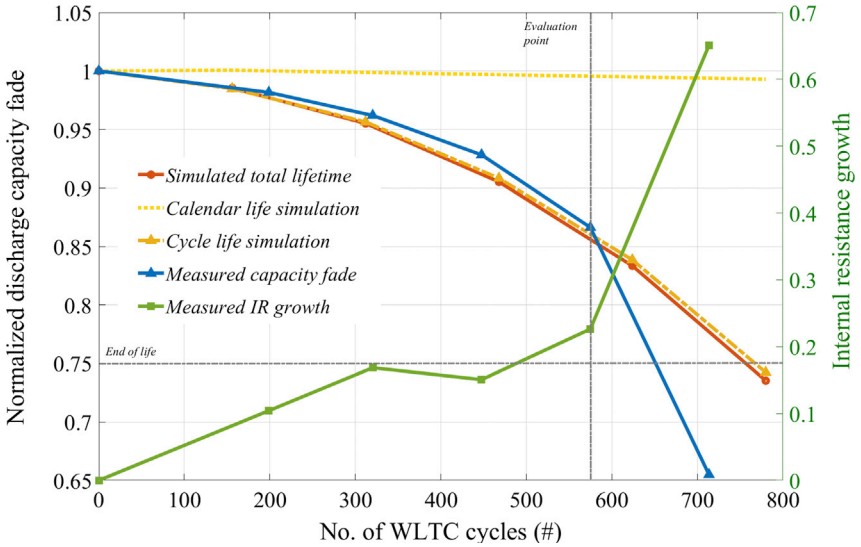

Figure 6. Semi-empirical model validation for dynamic WLTC profile

DISCUSSION

Models' performance assessment

As a rule of thumb, any aging model should only be termed as validated when the model prediction is compared with a set of unknown inputs and results. The validation or the testing of the model performance ideally needs to be performed on a completely separate cell based on laboratory-level static or realistic dynamic conditions. In this work, long-term aging tests are designed for the validation of the developed models. Two separate cells are studied with the validation profiles as explained in the experimental section, whereas the rest of the 38 cells' aging outputs are used to construct or train the developed models. In the following sections, the validation results are reported by the profile types (WLTC or static) and the assessment is done based on different performance criteria.

Model comparison for dynamic WLTC

The semi-empirical model (SeM), the data-driven GPR, and the advanced NARXnet models are validated with the designed WLTC profile, which is based on a real-life scenario as explained in the "Data generation" section. The dynamic currents are fed to the SeM model to simulate the life until the capacity fade reaches the EoL criterion (SoH<75%). The cycle life and calendar life scripts of the model (as shown in Figure 3) analyze the split current of load and non-load situations, respectively, and process the parameterized conditions based on mathematical equations. Figure 6 displays the simulated battery life against the measured capacity fade, which is also found to be related to the IR growth.

The number of performed WLTC cycles is adjusted with a factor of 1.3 as an 80% operating window is considered for dynamic cycling, while the model is based on full equivalent DoD cycling. Rainflow counter is used to separate the degradation parameters from signals such as DoD and SoC so that the cycling script can consider all the crucial impacts. Hence, the calendar life script is simulated taking extra rest into account. The model prediction results in 0.99 RMSE without considering the last data point, which can be regarded as unwanted electrochemical phenomena or an indication of battery failure. It clearly shows the dependency on the increased resistance of the battery termed as the capacity degradation knee point (Fermín-cueto et al., 2020). As only the cycling operating conditions are considered for the parameterization of the SeM, the model response could not capture the sudden degradation toward the EoL. This can be regarded as the limitation of the model, which can be further improved with the inclusion of IR measurement.

However, in the case of data-driven models, the number of WLTC cycles needs to be readjusted because the training data includes the conditional number (as per the test matrix) of cycles. Authors have found a relationship between the capacity fade rate and the IR growth for dynamic WLTC cycling.

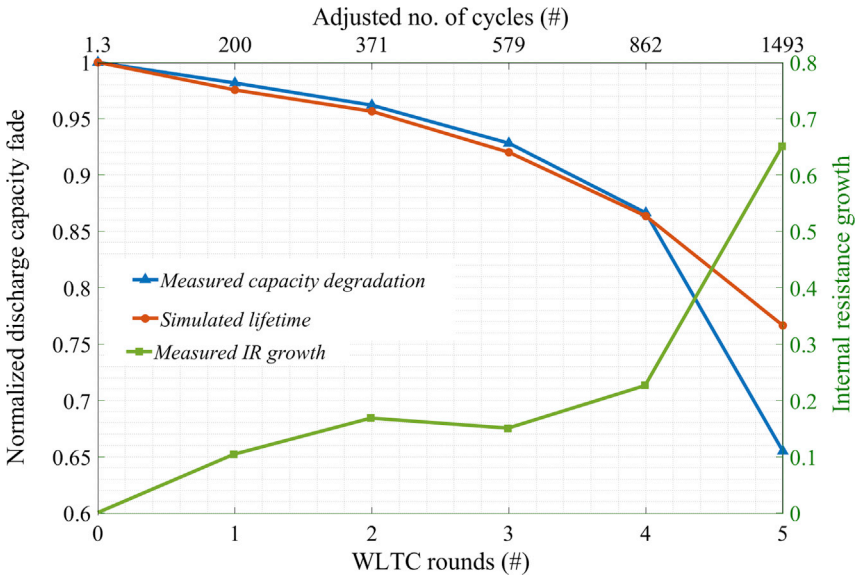

Figure 7. Data-driven GPR model validation for dynamic WLTC profile

$$C_{adj} = k * C_{n-1}\left(1 + \sum_{i=1}^{n} IR\right) \quad \text{(Equation 10)}$$

In this equation, C_{adj} is the adjusted number of cycles; k is the full DoD adjustment factor, which is 1.3 (calculated against DoD Ah); C_{n-1} is the performed WLTC cycles; and i denotes n number of iteration rounds (WLTC). The training process of the GPR model includes a total of eight aging features, which concedes the maximum computational effort. The trained model is then tested for the dynamic profile resulting in a very accurate 0.05 RMSE prediction. Once again, the capacity fade is underestimated toward the end of life, which is related to the high resistance growth. The model can be further improved with more fundamental battery characteristic (i.e., direct voltage, IR measurement, etc.) inputs to capture the EoL trend. Figure 7 shows how close the output response of the GPR model is compared with the actual capacity decay during most of the period.

The advanced NARXnet model has shown the best performance when it is validated against the dynamic WLTC cycles. A second-order polynomial fitting is used at first to generate test data points by interpolating the number of WLTC rounds. These calculated data points (as named) are then tested with the trained NARX model, and a precise 0.01 RMSE value is achieved. Figure 8 clearly shows the edge of the NARX model over the other models. The black box-type NARX model shows the capability of capturing the uncertain dynamicity of the investigated battery cell at EoL that other models could not.

Table 1 lists the model performances of the developed semi-empirical and data-driven models. The NARX model outperforms the GPR model and the SeM in terms of accuracy; however, the training process and data pre-processing of data-driven models require a significant amount of computational effort that can be compromised to the accuracy. The compared computational cost refers to the averaged running time of SeM's simulation and the training time of GPR's and NARXnet's data processing. All the simulation, training, and testing of the models are conducted with Intel Core i7-6820HQ (at 2.70GHz) processor and 16 GB (2,133 MHz) speed.

Static profile validation of ML models

Besides the dynamic WLTC validation, the static profile is selected to test both the trained ML models. To have a concrete validation, each cycle discharge capacity is simulated in comparison with the measured value.

Figure 9 shows the GPR model performance that is trained with several cycling and relaxation input parameters. The constant-current and constant-voltage (CCCV) condition used for this validation type is a separate profile and cycled with a new cell. The tested model performs quite accurately with a 0.89 RMSE

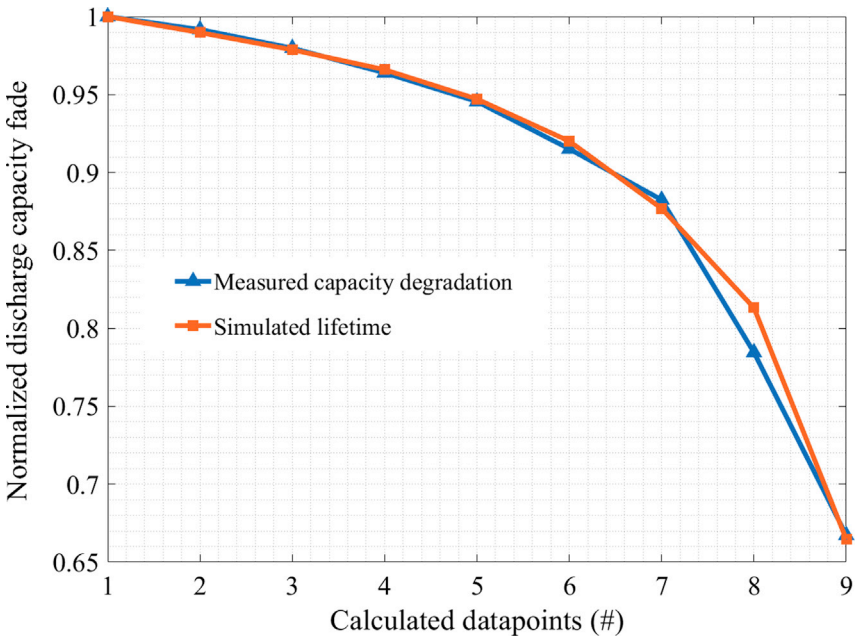

Figure 8. ANN model validation for dynamic WLTC profile considering intermediate data points

predicting each capacity value per cycle. The simulation curve overfits in the first cycling phase (up to 120 cycles) and underestimates in the second with various spikes related to the temperature rise (inserted axes). Hence, the model could not capture capacity gain during the start of the second phase, which is mainly because of GPR's limitation in predicting capacity regeneration (Liu et al., 2013). This is a crucial limitation that gets accumulated in the total model error. The slow training process of GPR can be compromised by good model accuracy.

On the contrary, the training of the NARX model is much faster than the GPR, although using a similar training dataset. Based on the training data, the trained model has responded with a 0.59 MSE (MSE is a without root version of RMSE) and 0.67 MSE for training and testing. However, it shows an excellent agreement between the target measurement and the test response with a 0.34 RMSE when it is validated with the static profile results. Figure 10 shows the capacity decay during the lifetime with error distribution. The tested model performance depicts underestimation only toward the EoL, which means an excellent agreement during the majority of the aging period proving the model's high competency. Table 2 compares the ML model performances tested for a static profile. The NARX model outperforms the GPR in terms of accuracy and computational effort. It can also capture the capacity regeneration after a rest period (inserted axis), which proves the robustness of using advanced algorithms.

Evaluation and assessment

The modeling of battery life has several challenges to overcome such as accuracy, computational effort, model complexity, etc. A robust and efficient aging model not only explains the battery degradation behavior but also helps to perform prognosis and diagnosis. Thus, it is crucial to select a suitable methodology to predict the capacity decay during the whole life. In this work, three different lifetime models (SeM, GPR, NARX) have been developed and compared on similar terms to provide a valid assessment of the

Table 1. Model assessment of dynamic validation based on the normalized capacity fade

	Semi-empirical model	GPR model	NARX model
RMSE	0.9916	0.0458	0.0099
MAE	0.8016	0.0253	0.0053
Simulation/training time	14 s	213 s	<1 s

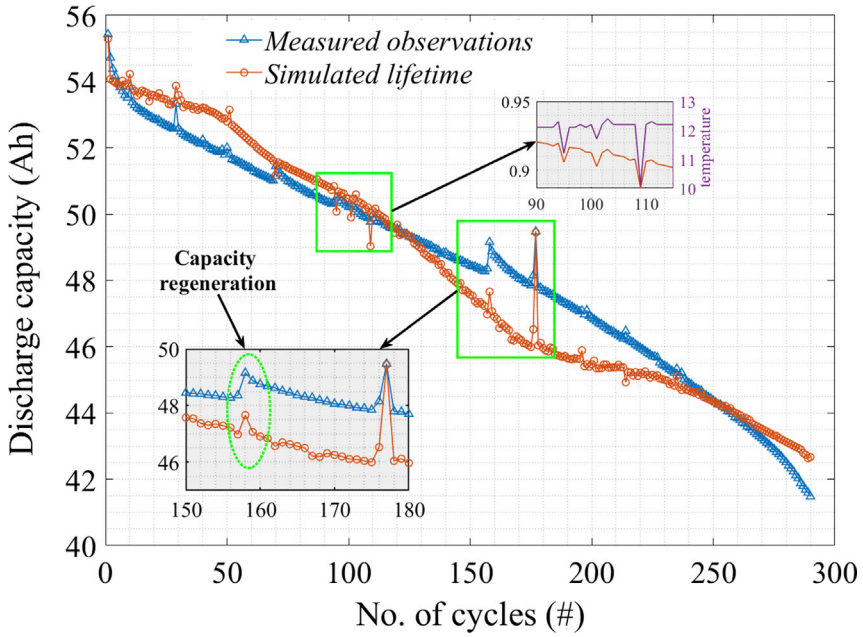

Figure 9. GPR model validation with static CCCV profile

performances. A comprehensive NMC aging dataset is used to construct and/or train all the models besides validating them with an unknown set of measurements.

All the models have shown quite accurate results in predicting capacity degradation, resulting in a very low RMSE value (<1). The GPR shows better results in dynamic profile validation; however, the NARX model performs better than the GPR in static profile validation. The NARX model can be considered as the best performing model overall among all in terms of accuracy. It also requires the least amount of computational effort when compared with the GPR and the SeM (simulation). The possible reasons for the better

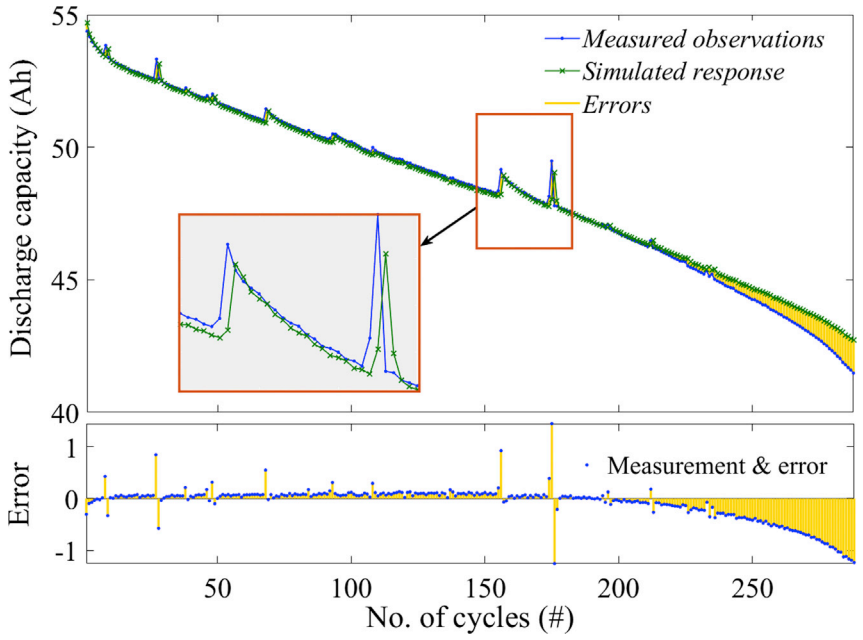

Figure 10. NARX model validation with static CCCV profile

Table 2. Model assessment of static validation based on relative capacity degradation

	GPR model	NARX model
RMSE	0.8922	0.3413
MAE	0.7192	0.0083
Simulation/training time	213 s	<1 s

performing NARXnet could be the learning and adapting ability of the algorithm from the training data, which distinguishes it from the kernel-dependent GPR and fitting equation-based SeM. The huge amount of experimental data has further helped the ANN model to perform better.

The models require an extensive amount of measurement data, which is considered as standard in this work. However, the rigorous task of data processing is significant on top of data generation, which is regarded as conventional as well. Regarding model complexity, SeM is a lighter model as it is represented by simple fitting equations fitting cycling, and calendar life degradation paths, separately. ML models are more complex as advanced algorithms are used in the training process. Besides, the GPR and NARX models follow black-box modeling methodology, which has no knowledge of the battery physical-chemical events. On the other hand, semi-empirical can still represent a little insight into the degradation mechanism following established algorithms like the Arrhenius equation for calendar life fade.

All the compared models can be used as an online prognosis tool implemented in the battery management system. However, the simplicity of SeM puts it ahead of other complex models in this regard. The number of processed parameters plays a major role, which requires memory and computational considerations, especially for model training. The trained ML models based on historical data can continuously improve by learning from the real-life information if implemented in the local device or via cloud simulation. However, the implementation cost, communication systems, computational delay, etc., are the crucial challenges that need to be compromised to get the accurate battery states (SoC, lifetime). On the contrary, fewer input parameters make SeM an undemanding choice with a higher RMSE error.

Figure 11 displays the investigated lifetime modeling methodologies comparison in terms of key assessment criteria. However, the existing limitations still require intensive research in this field, especially,

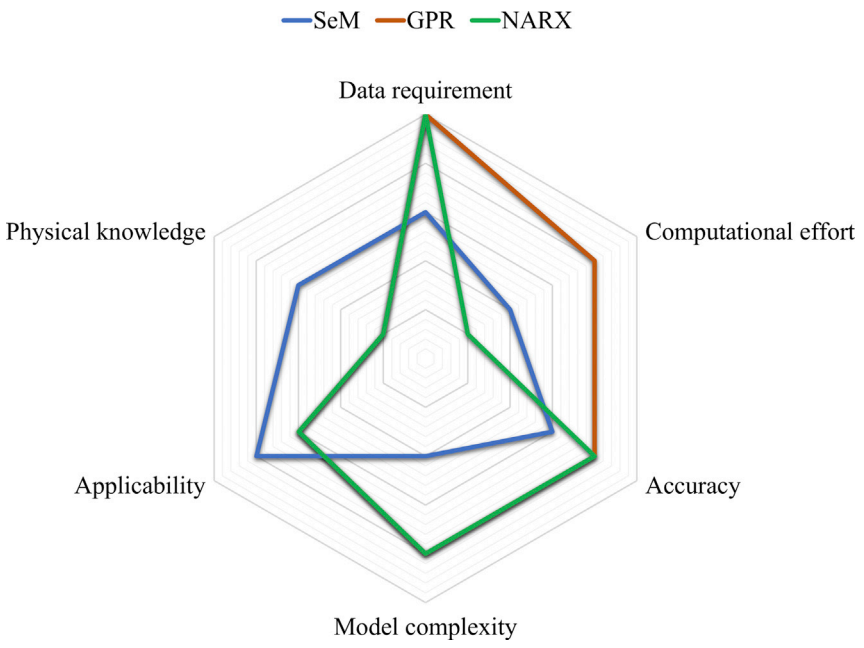

Figure 11. Radar chart for the performance evaluation of the investigated models (outer lines mean higher assessment)

when there are varieties of Li-ion battery chemistries available of different properties. The highly nonlinear characteristics of these batteries are the main obstacle to achieving a universal lifetime model. Both the technology-specific electrochemical models and performance-fitted SeMs are defined to follow a particular degradation path. Thus, advanced algorithms and self-learning models can be a solution to future lifetime modeling compromising the cost and computational effort. Hence, further material development can also restrict nonlinearity meaning that a simple model like SeM can be implemented with high accuracy.

CONCLUSION

The lifetime of Li-ion batteries is the key challenge to achieve sustainable battery performance. The application-specific usage dominates the degradation path, and an accurate aging prediction is still a challenge. The precise forecasting of the battery life has a far-reaching consequence, which can help to understand the battery behavior under certain circumstances and perform diagnosis accordingly. In this research work, several lifetime models are developed following different methodologies, and model performances are compared with each other. The assessment is validated by using a common training dataset and tested/simulated on completely new cells. It has been found that the data-driven models are more accurate than the SeM. The NARX model is the most precise with a 0.01 RMSE when validated with a WLTC profile requiring less than a second for training. On the other hand, the SeM is the simplest of all that can predict the capacity fade with 0.99 RMSE during the whole life. Hence, the data-driven ML models are validated with a static cycling profile where the NARX model once again shows the best performance scoring a very accurate 0.34 RMSE. Moreover, the constructed models are scrutinized and differentiated in terms of data requirement, model complexity, computational effort, applicability, etc., and the pros and cons are explained. It can be concluded from the discussions that no model is perfect; nevertheless, the best can be useful. The outcome of the evaluation in this work would help the research community to choose the most suitable lifetime modeling methodology according to the purpose. Hence, the best model methodology is aimed to flourish to achieve a chemistry-neutral approach following future research prospects (BATTERY 2030+, 2020).

Limitations of the study

All the developed lifetime models in this work can be used as an efficient tool for the investigated NMC cell. However, the developed models could be further optimized to achieve the best possible results. Unfortunately, the models could not be verified against the static profile, which is a scope of improvement of the work. Also, the models' adaptability to other types of battery technologies is a challenge. So, more optimization and validation by a quality dataset could be done in the future to further improve the model's performance and robustness.

Resource availability

Lead contact

Further requests for information should be directed and will be handled by the corresponding author and lead contact, Md Sazzad Hosen (md.sazzad.hosen@vub.be).

Materials availability

The study did not generate new materials.

Data and code availability

The data generated in this study could not be shared due to confidentiality; however, the ML modeling codes supporting the work are available from the lead contact upon request.

METHODS

All methods can be found in the accompanying Transparent methods supplemental file.

SUPPLEMENTAL INFORMATION

Supplemental information can be found online at https://doi.org/10.1016/j.isci.2021.102060.

ACKNOWLEDGMENTS

The battery lifetime test campaign and the full work has been done in the Battery Innovation Center of MOBI Research Group. Furthermore, we acknowledge "Flanders Make" for their support to the research group.

AUTHOR CONTRIBUTION

Conceptualization, Methodology, Software, Validation, Formal analysis, Investigation, Data Curation, Writing – Original Journal Draft, M.S.H.; Writing – Review & Editing: J.J., J.V.M., and M.B.; Supervision, M.B.

DECLARATION OF INTERESTS

The authors declare no competing interests.

Received: November 21, 2020
Revised: December 27, 2020
Accepted: January 12, 2021
Published: February 19, 2021

REFERENCES

Barré, A., Deguilhem, B., Grolleau, S., Gérard, M., Suard, F., and Riu, D. (2013). A review on lithium-ion battery ageing mechanisms and estimations for automotive applications. J. Power Sources *241*, 680–689.

Batteries2020 (2013). http://www.batteries2020.eu/.

BATTERY 2030+ (2020). https://battery2030.eu/.

BATTLE (2013). http://etec.vub.ac.be/battle/.

Berecibar, M., Gandiaga, I., Villarreal, I., Omar, N., Van Mierlo, J., and Van den Bossche, P. (2016). Critical review of state of health estimation methods of Li-ion batteries for real applications. Renew. Sustainable Energy Rev. *56*, 572–587.

Birkl, C.R., Roberts, M.R., McTurk, E., Bruce, P.G., and Howey, D.A. (2017). Degradation diagnostics for lithium ion cells. J. Power Sources *341*, 373–386.

Boussaada, Z., Curea, O., Remaci, A., Camblong, H., and Mrabet Bellaaj, N. (2018). A nonlinear autoregressive exogenous (NARX) neural network model for the prediction of the daily direct solar radiation. Energies *11*, 620.

Broussely, M., Herreyre, S., Biensan, P., Kasztejna, P., Nechev, K., and Staniewicz, R.J. (2001). Aging mechanism in Li ion cells and calendar life predictions. J. Power Sources *97-98*, 13–21.

Cheng, Y., Lu, C., Li, T., and Tao, L. (2015). Residual lifetime prediction for lithium-ion battery based on functional principal component analysis and Bayesian approach. Energy *90*, 1983–1993.

Christensen, J., and Newman, J. (2005). Cyclable Lithium and Capacity Loss in Li-Ion Cells*152* (J. Electrochem. Soc.), pp. 818–829.

de Hoog, J., Timmermans, J.M., Ioan-Stroe, D., Swierczynski, M., Jaguemont, J., Goutam, S., Omar, N., Van Mierlo, J., Van Den Bossche, P., et al. (2017). Combined cycling and calendar capacity fade modeling of a Nickel-Manganese-Cobalt Oxide Cell with real-life profile validation. Appl. Energy *200*, 47–61.

Duvenaud, D., Lloyd, J.R., Grosse, R., Tenenbaum, J.B., Ghahramani, Z., et al. (2013). Structure discovery in nonparametric regression through compositional kernel search. Int. Conf. Machine Learn. *28*, 1166–1174.

Ecker, M., Gerschler, J.B., Vogel, J., Käbitz, S., Hust, F., Dechent, P., and Sauer, D.U. (2012). Development of a lifetime prediction model for lithium-ion batteries based on extended accelerated aging test data. J. Power Sources *215*, 248–257.

Ecker, M., Nieto, N., Käbitz, S., Schmalstieg, J., Blanke, H., Warnecke, A., and Sauer, D.U. (2014). Calendar and cycle life study of Li(NiMnCo)O2-based 18650 lithium-ion batteries. J. Power Sources *248*, 839–851.

Ecker, M., Shafiei Sabet, P., and Sauer, D.U. (2017). Influence of operational condition on lithium plating for commercial lithium-ion batteries - electrochemical experiments and post-mortem-analysis. Appl. Energy *206*, 934–946.

Eddahech, A., Briat, O., Bertrand, N., Delétage, J.-Y., and Vinassa, J.-M. (2012). Behavior and state-of-health monitoring of Li-ion batteries using impedance spectroscopy and recurrent neural networks. Int. J. Electr. Power Energy Syst. *42*, 487–494.

Fermín-cueto, P., McTurk, E., Allerhand, M., Medina-Lopez, E., Anjos, M.F., Sylvester, J., dos Reis, G., et al. (2020). Energy and AI Identification and machine learning prediction of knee-point and knee-onset in capacity degradation curves of lithium-ion cells. Energy and AI *1*, 100006.

He, W., Pecht, M., Flynn, D., and Dinmohammadi, F. (2018). A physics-based electrochemical model for lithium-ion battery state-of-charge estimation solved by an optimised projection-based method and moving-window filtering. Energies *11*, 2120.

Dai, H., Zhang, X., Gu, W., Wei, X., and Sun, Z. (2013). A semi-empirical capacity degradation model of ev li-ion batteries based on eyring equation. IEEE VPPC *2013*, 36–40, 2013 9th IEEE Vehicle Power and Propulsion Conference.

de Hoog, J., Jaguemont, J., Nikolian, A., Van Mierlo, J., Van Den Bossche, P., and Omar, N. (2018). A combined thermo-electric resistance degradation model for nickel manganese cobalt oxide based lithium-ion cells. Appl. Therm. Eng. *135*, 54–65.

Hosen, M.S., Karimi, D., Kalogiannis, T., Pirooz, A., Jaguemont, J., Berecibar, M., and Van Mierlo, J. (2020). Electro-aging model development of nickel-manganese-cobalt lithium-ion technology validated with light and heavy-duty real-life profiles. J. Energy Storage *28*, 101265.

Hu, X., Xu, L., Lin, X., Pecht, M., et al. (2020). Battery lifetime prognostics. Joule *2019*, 1–37.

Hu, X., Zou, C., Zhang, C., Li, Y., et al. (2017). Technological developments in batteries: a survey of principal roles, types, and management needs. IEEE Power Energ. Mag. *15*, 20–31.

Hussein, A.A. (2015). Capacity fade estimation in electric vehicle Li-ion batteries using artificial neural networks. IEEE Trans. Ind. Applicat. *51*, 2321–2330.

Jafari, M., Khan, K., and Gauchia, L. (2018). Deterministic models of Li-ion battery aging: it is a matter of scale. J. Energy Storage *20*, 67–77.

Käbitz, S., Gerschler, J.B., Ecker, M., Yurdagel, Y., Emmermacher, B., André, D., Mitsch, T., and Sauer, D.U. (2013). Cycle and calendar life study of a graphite|LiNi1/3Mn1/3Co1/3O2 Li-ion high energy system. Part A: full cell characterization. J. Power Sources *239*, 572–583.

Li, Y., Liu, K., Foley, A.M., Zülke, A., Berecibar, M., Nanini-Maury, E., Van Mierlo, J., Hoster, H.E., et al. (2019). Data-driven health estimation and lifetime prediction of lithium-ion batteries : a review. Renew. Sustainable Energy Rev. *113*, 109–254.

Li, Y., Zou, C., Berecibar, M., Nanini-Maury, E., Chan, J.C.-W., van den Bossche, P., Van Mierlo, J., and Omar, N. (2018). Random forest regression for online capacity estimation of lithium-ion batteries. Appl. Energy *232*, 197–210.

Lipu, M.S.H., Hannan, M.A., Hussain, A., Saad, M.H.M., Ayob, A., and Blaabjerg, F. (2018). State of charge estimation for lithium-ion battery using recurrent NARX neural network model based lighting search algorithm. IEEE Access *6*, 28150–28161.

Liu, K., Hu, X., Wei, Z., Li, Y., Jiang, Y., et al. (2019). Modified Gaussian process regression models for cyclic capacity prediction of. IEEE Trans. transportation electrification *7782*, 2332–7782.

Liu, K., Li, Y., Hu, X., Lucu, M., Widanage, W.D., et al. (2020). Gaussian process regression with automatic relevance determination kernel for calendar aging prediction of lithium-ion batteries. IEEE Trans. Ind. Inform. *16*, 3767–3777.

Liu, D., Pang, J., Zhou, J., Peng, Y., and Pecht, M. (2013). Prognostics for state of health estimation of lithium-ion batteries based on combination Gaussian process functional regression. Microelectronics Reliability *53*, 832–839.

Lucu, M., Martinez-Laserna, E., Gandiaga, I., Liu, K., Camblong, H., Widanage, W.D., and Marco, J. (2020). Data-driven nonparametric Li-ion battery ageing model aiming at learning from real operation data - Part B: cycling operation. J. Energy Storage *30*, 101410.

Liu, J., Saxena, A., Goebel, K., Saha, B., Wang, W., et al. (2010). An Adaptive Recurrent Neural Network for Remaining Useful Life Prediction of Lithium-Ion Batteries (Annual Conference of the Prognostics and Health Management Society), pp. 0–9.

Lucu, M., Gandiaga, I., and Camblong, H. (2018). Review article A critical review on self-adaptive Li-ion battery ageing models. J. Power Sources *401*, 85–101.

Member, S., and Ibe-ekeocha, C.C. (2017). State of charge and state of health estimation for lithium batteries using recurrent neural networks. IEEE Trans. vehicular Technol. *66*, 8773–8783.

Nuhic, A., Terzimehic, T., Soczka-Guth, T., Buchholz, M., and Dietmayer, K. (2013). Health diagnosis and remaining useful life prognostics of lithium-ion batteries using data-driven methods. J. Power Sources *239*, 680–688.

Nykvist, B., and Nilsson, M. (2015). Rapidly falling costs of battery packs for electric vehicles. Nat. Clim. Change *5*, 100–103.

Omar, N., Monem, M.A., Firouz, Y., Salminen, J., Smekens, J., Hegazy, O., Gaulous, H., Mulder, G., Van den Bossche, P., Coosemans, T., and Van Mierlo, J. (2014). Lithium iron phosphate based battery – assessment of the aging parameters and development of cycle life model. Appl. Energy *113*, 1575–1585.

Palacín, M.R. (2018). Understanding ageing in Li-ion batteries: a chemical issue. Chem. Soc. Rev. *47*, 4924–4933.

Palacín, M.R., and Guibert, A.de (2016). Why Do Batteries Fail?, pp. 574–581.

Rasmussen, C.E. (2003). Gaussian processes in machine learning. In Summer School on Machine Learning, Olivier Bousquet, ed. (Springer), pp. 63–71.

Richardson, R.R., Osborne, M.A., and Howey, D.A. (2017). Gaussian process regression for forecasting battery state of health. J. Power Sources *357*, 209–219.

Richardson, R.R., Osborne, M.A., and Howey, D.A. (2019). Battery health prediction under generalized conditions using a Gaussian process transition model. J. Energy Storage *23*, 320–328.

Saha, B., and Goebel, K. (2007). Battery Data Set. NASA AMES Prognostics Data Repository (NASA AMES prognostics data repository).

Saha, B., Poll, S., Goebel, K., Christophersen, J., et al. (2007). An Integrated Approach to Battery Health Monitoring (IEEE Autotestcon), pp. 646–653.

Scrosati, B., and Garche, J. (2010). Lithium batteries: status, prospects and future. J. Power Sources *195*, 2419–2430.

Severson, K.A., Attia, P.M., Jin, N., Perkins, N., Jiang, B., Yang, Z., Chen, M.H., Aykol, M., Herring, P.K., Fraggedakis, D., Bazant, M.Z., et al. (2019). Data-driven prediction of battery cycle life before capacity degradation. Nat. Energy *4*, 383–391, https://doi.org/10.1038/s41560-019-0356-8.

Su, L., Zhang, J., Huang, J., Ge, H., Li, Z., Xie, F., and Liaw, B.Y. (2016). Path dependence of lithium ion cells aging under storage conditions. J. Power Sources *315*, 35–46.

Suri, G., and Onori, S. (2016). A control-oriented cycle-life model for hybrid electric vehicle lithium-ion batteries. Energy *96*, 644–653.

Wang, D., Kong, J.-Z., Zhao, Y., and Tsui, K.-L. (2019). Piecewise model based intelligent prognostics for state of health prediction of rechargeable batteries with capacity regeneration phenomena. Measurement *147*, 106836.

Wang, F.-K., and Mamo, T. (2018). A hybrid model based on support vector regression and differential evolution for remaining useful lifetime prediction of lithium-ion batteries. J. Power Sources *401*, 49–54.

Wu, J., Zhang, C., and Chen, Z. (2016). An online method for lithium-ion battery remaining useful life estimation using importance sampling and neural networks. Appl. Energy *173*, 134–140.

Xing, Y., Ma, E.W., Tsui, K.L., Pecht, M., et al. (2013). Microelectronics Reliability an ensemble model for predicting the remaining useful performance of lithium-ion batteries. Microelectronics Reliability *53*, 811–820.

Yang, X.-G., Leng, Y., Zhang, G., Ge, S., and Wang, C.-Y. (2017). Modeling of lithium plating induced aging of lithium-ion batteries: transition from linear to nonlinear aging. J. Power Sources *360*, 28–40.

Zhu, S., Zhao, N., and Sha, J. (2019). Predicting battery life with early cyclic data by machine learning. Energy Storage, 1–5.

iScience, Volume *24*

Supplemental Information

Battery lifetime prediction and performance assessment of different modeling approaches

Md Sazzad Hosen, Joris Jaguemont, Joeri Van Mierlo, and Maitane Berecibar

Supplementary Information

Transparent Methods

In this research work, an aging dataset of 40 NMC cells is used which has been generated during one and a half years of lifetime characterization. The discharge nominal capacity of this high-energy cell varies between 59-62 Ah at room temperature. This plentiful and comprehensive dataset is produced by using PEC manufactured ACT type battery cyclers and the ambient temperature is controlled by CTS made climate chambers.

Data generation

The commercial battery cells used in this research are cycled with a constrained structure to emulate realistic scenarios. Every cell was sandwiched between two aluminum plates and screwed to ensure safety and improved performance (Wünsch, Kaufman and Uwe, 2019). The test campaign consists of battery characterization both at the beginning of life (BoL) and the end of life (EoL) while a hybrid plan of cycling and rest phases dominates the aging procedure. The self-explanatory Figure 11 shows the use of combined cycling and relaxation phases which were used to age the batteries. The test end criterion in this work is considered when the SoH of the cell falls below 75% of the nominal discharged capacity.

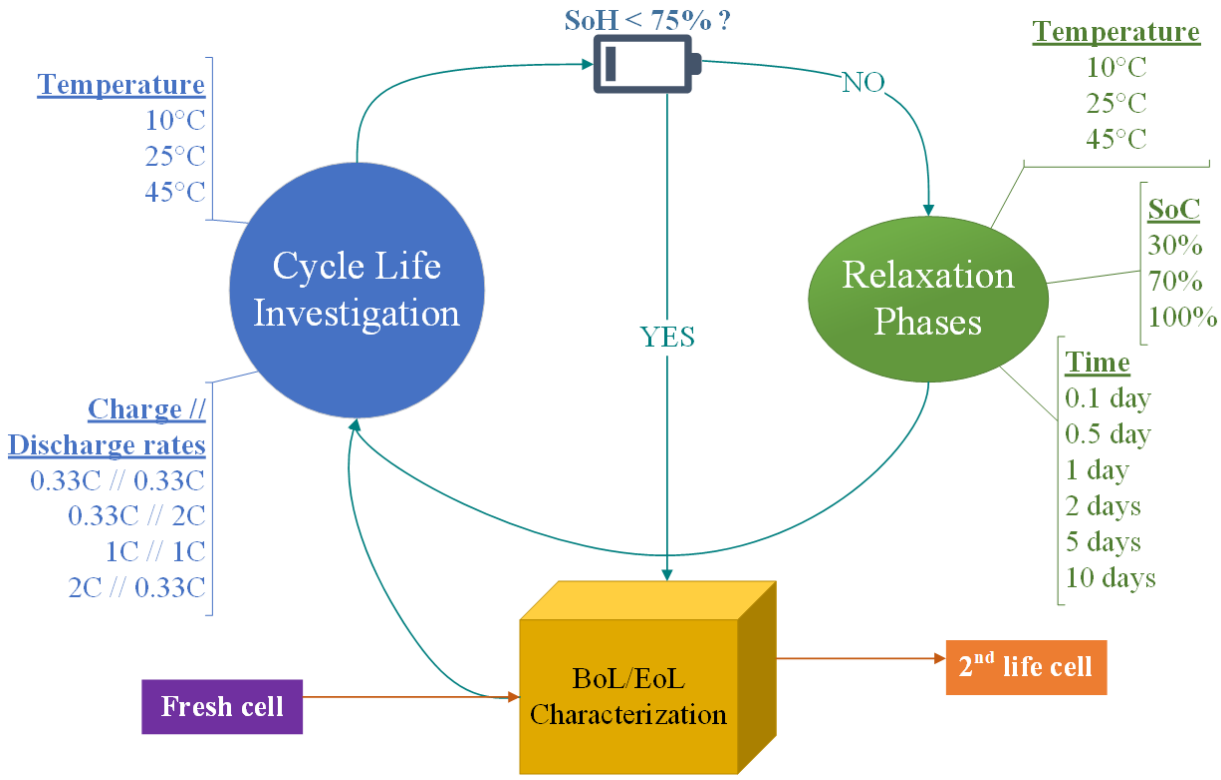

Figure S1: Battery aging test flow chart. The investigated cells are cycled as per this test procedure. Related to the results published in Figure 2.

All but selective BoL/EoL characterization data is used to identify the nominal parameters of the cell. The capacity test was performed with the C/3 rate only at BoL and at EoL. All the cycling batteries were cycled following the constant-current and constant voltage (CCCV) procedure in charge direction and the constant-current (CC) procedure in discharge direction according to the specified test conditions. A 10-minute rest was employed between every charge and discharge step. Due to the high repeatability of the cell, one cell per condition was studied. The batteries were cycled typically 50 times within the operating voltage region (100% DoD) in a single round and the last cycle discharge capacity is used as the actual capacity. After every cycling round, the required rest was provided to every cell in terms of temperature, SoC, and duration. In this way, 38 different combinations of operating parameters were studied in the unique experimental phase. The circle of cycling and relaxation was continued until the cell reaches the EoL which is calculated by the following equation.

$$SoH_i = (Q_{i*j} / Q_{i*1}) * 100\% \quad (1)$$

In equation (1), i refers to the cell number, Q is the discharge capacity and j is the performed number of cycles. The very first cycle capacity is considered as the nominal value in the calculation. Besides aging tests, two types of validation tests were performed on separate cells. The static test was cycled twice with 1C charge-discharge rate at 10°C for 150 full cycles before a 1-day rest at 30% SoC at room temperature in between. The same CCCV charge and CC discharge procedures are followed for the static test. On the contrary, the dynamic profile is designed based on an on-road vehicle (AUDI e-Tron) adjusting the WLTC currents, accordingly. The test was performed within 80% DoD (operating window) for 12 days at 10°C before resting it at 70% SoC and room temperature after every WLTC round. A capacity and resistance checkup were performed after every WLTC round to track the SoH of the cell.

Supplemental References

Wünsch, M., Kaufman, J. and Uwe, D. (2019) 'Investigation of the influence of different bracing of automotive pouch cells on cyclic lifetime and impedance spectra', *Journal of Energy Storage*, 21(November 2018), pp. 149–155.